BRILL

CONTRIBUTIONS TO ZOOLOGY 94 (2025) 64–97

CTOZ

brill.com/ctoz

Shell chirality and phylogeography of land snail *Satsuma batanica* species group (Gastropoda: Stylommatophora: Camaenidae)

Chung-Chi Hwang | ORCID: 0000-0002-4780-4909
Department of Life Sciences, National University of Kaohsiung, Kaohsiung, 811, Taiwan

Mang-Jye Ger | ORCID: 0000-0002-9016-6172
Department of Life Sciences, National University of Kaohsiung, Kaohsiung, 811, Taiwan

Shu-Ping Wu | ORCID: 0000-0001-6764-1118
Department of Earth and Life Sciences, University of Taipei, Taipei, 100234, Taiwan
shupingwu@ntu.edu.tw; spwu@utaipei.edu.tw

RECEIVED 10 APRIL 2024; REVISED 29 AUGUST 2024; ACCEPTED 6 SEPTEMBER 2024; PUBLISHED ONLINE 27 SEPTEMBER 2024; PUBLISHED IN ISSUE 13 JANUARY 2025
EDITOR: DANWEI HUANG

Abstract

Chirality has been recognised as a potentially important mechanism in the speciation of land snails because it leads to reproductive isolation between individuals with different coiling directions. The *Satsuma batanica* species group comprises the sinistral *S. batanica* and the dextral *S. bacca*, despite the observed sympatric distributions of the two chiral morphs. This study examines the population structure, phylogeographic history and taxonomy of the species group by analyzing mitochondrial CO1 gene sequences. A total of 127 haplotypes were identified from 367 individuals collected from 39 locations. The phylogenetic trees, constructed using Bayesian inference and maximum likelihood methods, along with the median-joining network, identified 14 clades. The reconstructed ancestral states indicate that the most recent common ancestor of the *S. batanica* species group was sinistral. The frequent occurrence of the dextral morph, the shared haplotype, the sympatric distribution, and the co-occurrence of the two chiral morphs within the same phylogenetic clades recovered here do not support reproductive isolation and single-gene speciation based on chiral differences. All the names belonging to the *S. batanica* species group are considered synonyms because of their molecular and morphological similarities. This species is estimated to have originated approximately 615 thousand years ago from the

Published with license by Koninklijke Brill BV | DOI:10.1163/18759866-BJA10071
© CHUNG-CHI HWANG ET AL., 2024 | ISSN: 1383-4517 (print) 1875-9866 (online)
This is an open access article distributed under the terms of the CC BY 4.0 license.

northern margin of its current distribution. Two major genetic divergence stages occurred around 440 and 50–100 thousand years ago. The formation of ancient islands through orogenic activities is utilised to explain the phylogeographic history of the species.

Keywords

chirality – land snail – phylogeography – synonymy – taxonomy

Introduction

Land snails of different coiling directions, dextral and sinistral, are thought to be unable to copulate successfully due to prezygotic isolation caused by mismatches associated with the genitalia and behaviour (Asami et al., 1998; Gittenberger et al., 2012). Although behavioural evidence (Johnson, 1982; Ueshima & Asami, 2003; Richards et al., 2017) also suggests congeneric species of different chiralities are capable of mating, a significantly lower frequency of copulation success, as well as a lower number of laid eggs and hatched offspring were observed in inter-chiral mating compared to intra-chiral mating for *Bradybaena similaris* (Ueshima & Asami, 2003) and *Partula suturalis* (Johnson, 1982). Molecular phylogenetic studies of *Euhadra* and *Satsuma* species (Ueshima & Asami, 2003; Davison et al., 2005; Hoso et al., 2010) demonstrate repeated evolution in chiral directions between species within the same genus. The hypothesis of single-gene speciation, which posits that sympatric speciation occurs due to changes in a single gene (Orr, 1991), has long been debated in relation to the chirality of shell coiling mentioned above. This type of speciation is considered unlikely due to the reproductive incompatibility of the new mutant, but it may occur when other facilitating factors are present (Davison et al., 2005; Hoso et al., 2010). A recent study (Richards et al., 2017) on the genetics of populations of two closely related species, the sinistral *E. quaesita* and dextral *E. aomoriensis*, shows that the two species exhibit gene flow between snails with opposite coiling directions.

The land snail genus *Satsuma* Adams, 1868 is distributed in East Asia, spanning Japan, Taiwan, southern China, and the Batan Islands of the Philippines (Minato, 1988; Schileyko, 2004; Hsieh et al., 2013; Wang et al., 2014; Adams & Reeve, 1850). The shells of *Satsuma* are notably diverse in shape, size, colour, chirality, and banding pattern (Kuroda & Habe, 1949; Azuma, 1995; Hsieh et al., 2013; Hoso et al., 2010). Different species of the genus were observed to exhibit strict terrestrial, semi-arboreal, or arboreal habits (Wu et al., 2008). The sinistral *S. batanica* (Adams & Reeve, 1850) and its subspecies, and the dextral *S. bacca* (Pfeiffer, 1866) are a species group primarily found in southern Taiwan, including the Hengchun Peninsula, Green Island, Lanyu Island (also known as Orchid Island and Botel Tobago Island), and the Batan

Islands (fig. 1). Shells in this group exhibit variations in size (shell width < 15–30 mm, shell height < 10–22 mm), shape (shell height/shell width = 0.62–0.85), colour (yellow to dark brown), chirality, and banding pattern (with three surrounding bands and one umbilical spot of varied width) (Kuroda, 1932; Chang, 1992; Hwang, 1995). The snails exhibit semi-arboreal behaviour; they crawl on trees during rainy seasons and hide in soil or rock crevices during dry seasons. Molecular phylogenetics (Hoso et al., 2010) indicates that the two species are sister taxa and closely related to species with geographical affinity in southern and eastern Taiwan. The dextral morph snails are distributed in the northwest of the Hengchun Peninsula, while the sinistral morph snails are widely distributed in the remaining areas mentioned above. Sympatric distributions of the two chiral morphs are observed in five locations (fig. 1). The four populations on the peninsula are located approximately on the distribution boundary of the two morphs. Secondary contact may have occurred here after the divergence of the two chiral morphs. The morphological variations and sympatric distributions provide an opportunity to examine the phylogeography among populations and speciation of the two species.

The Hengchun Peninsula, situated south of 22°30′N, is the most recently formed and southernmost landmass of Taiwan, due to the island was uplifted in the north first and then gradually uplifted southward due to the arc-continent collision that began around 6–5 million years ago (MYA; Huang et al., 2006). The highest peak and possibly the oldest landmass, Mt. Lilongshan, of the peninsula has uplifted from sea level since 2.6–3.5 MYA (Kao, 2020). The remainder of the peninsula is relatively young, having been uplifted since 1 MYA (Huang et al., 2006). The present West Hengchun Hills are estimated to have formed 120 thousand years ago (KYA) as coral reefs and were then uplifted as barrier islands, creating a lagoon environment between the barrier islands and the central Peninsula until the lagoon dried out in the Holocene (Giletycz et al., 2019). The two offshore islands, Green Island and Lanyu Island, along with Batan Island, are part of the northern Luzon Volcanic Arc. The two former islands are young volcanic formations that ceased erupting 1.5 MYA and 0.5 MYA (Huang et al., 2006). The southern part of Batan Island experienced early volcanic activity between 5.8–1.7 MYA (Sajona et al., 2000). These geologically young and isolated landmasses provide a unique opportunity for studying genetic divergence and speciation of biota at their early stages along the orogenic belt (Hall, 2002; Sibuet et al., 2002).

The current research aims to examine the possibility of recent contact between the two chiral morphs; to investigate the population structures of the snails; to infer the phylogeographic history of the species group on the geologically young landmass, and understand how the biota evolved on the island during its early stage of uplifting from sea level.

Material and methods

Sampling

Specimens were collected from 38 locations in Taiwan, primarily from the Hengchun Peninsula (fig. 1, table 1). Live

snails were drowned in water and then briefly fixed in hot water at 95 °C. Some specimens were prepared using the Niku-nuki method (Fukuda et al., 2008). Specimens were then preserved in 95% ethanol and stored at –20 °C.

Molecular analyses

Total DNA was extracted from the pedal muscle of ethanol-preserved specimens using the HotSHOT method (Truett et al., 2000). Molecular analyses were conducted using mitochondrial cytochrome oxidase subunit I (COI). Partial sequences of the COI gene were amplified using the universal primer pairs LCO1490/HCO2198 or LCO1490/C1N2191 (Folmer et al., 1994; Simon et al., 1994), with an annealing temperature of 45 °C. The amplification conditions were described in detail by Hwang et al. (2021). The amplicons were purified using a Genomics Universal DNA Purification kit (Genomics, Taiwan). Cycle sequencing was performed using the PCR primer and an ABI 3730XL automated sequencer. All sequence data are deposited in GenBank (table 1).

Genetic diversity and phylogenetic analyses

Chromatographs and sequences were reviewed, modified, and converted between formats using BIOEDIT 7.0.1. (Hall, 1999), and AliView 1.26 (Larsson, 2014). Sequences of *S. batanica* from the Batan Islands were obtained from GenBank (Batomalaque et al., 2013) and were included in the subsequent analyses. Sequences were aligned using MAFFT (Katoh & Standley, 2013) and subsequently trimmed at both the 5′ and 3′ ends to avoid missing sites. The saturation of base substitutions was assessed using Xia's method (Xia et al., 2003), implemented in DAMBE v.7.0.10 (Xia, 2018). Unique haplotypes were identified using DAMBE 7 (Xia, 2018).

The best-fit model of nucleotide substitution was determined for each codon using Model Finder (Kalyaanamoorthy et al., 2017) compiled in IQtree 1.6.12 (Nguyen et al., 2015) based on the Bayesian information criterion (BIC). The selected substitution model was applied in the Bayesian inference (BI) and maximum likelihood (ML) analyses. The BI analyses were conducted using the Markov chain Monte Carlo (MCMC) method implemented in MrBayes 3.2.6 (Ronquist et al., 2012). Four runs with eight independent chains were run on a computer, with sampling taking place every 2,000 generations, in order to estimate the posterior probability distribution. The analyses were considered to have reached stationarity when the average standard deviation of split frequencies fell below 0.0095 (using the option stoprule). The stationarity and convergence of the chains were assessed using Tracer v1.7.1 (Rambaut et al., 2018). The Markov chain was considered stationary when the effective sample sizes (ESS) for all parameters were greater than 200 in all analyses. The initial 25% of the total samples were discarded as burn-in. Subsequently, a majority-rule consensus tree was constructed, and the posterior probabilities (PP) for branches were calculated. Maximum likelihood (ML) analyses were conducted using IQtree 1.6.12 (Nguyen et al., 2015). Branch supports for ML tree were evaluated using ultrafast bootstrapping (Hoang et al., 2018) implemented in the IQ-TREE software. *Satsuma*

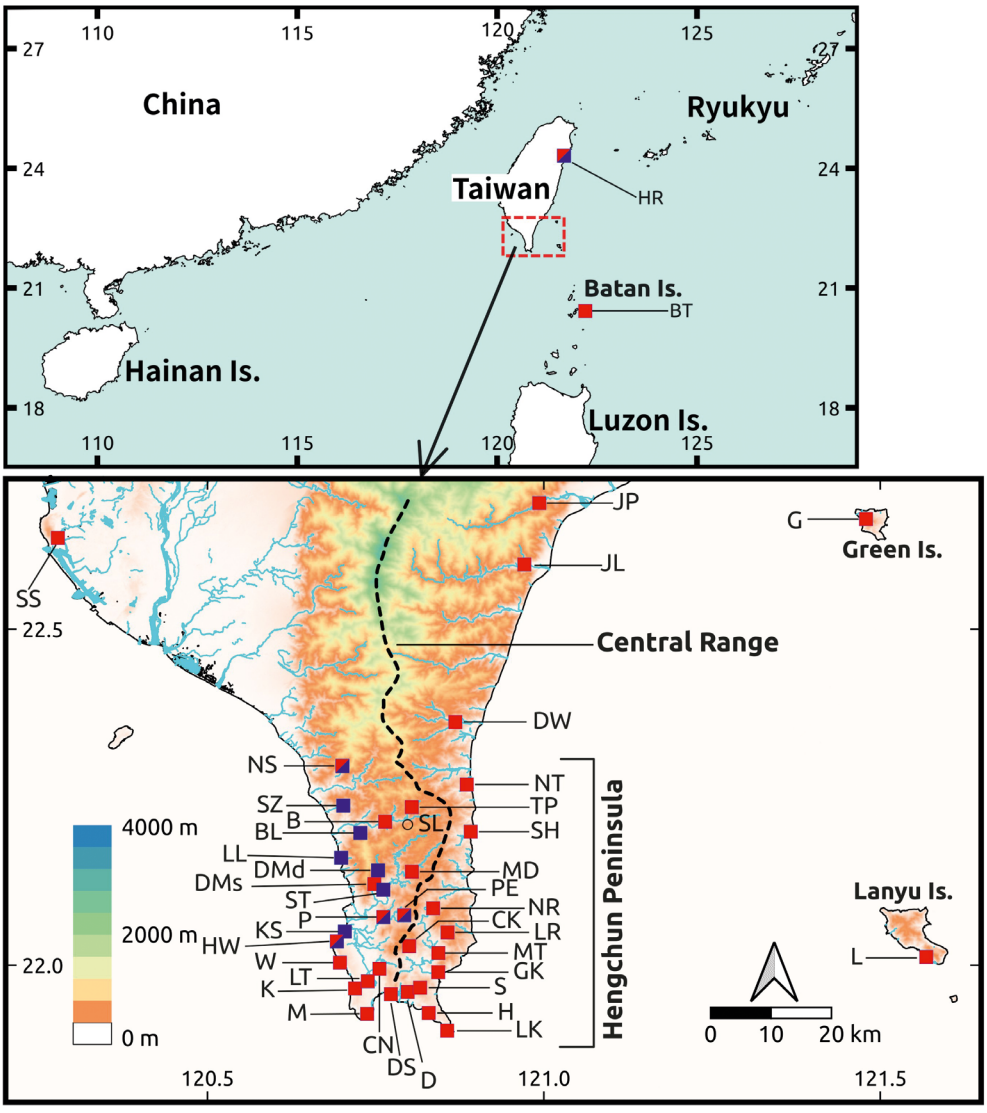


FIGURE 1 Sampling locations of *Satsuma batanica* species group in this study. The location codes for the sampling sites are detailed in table 1. The coloured square shows sinistral (red) and dextral (blue) shell chirality. The black dashed line indicates the ridge of the Central Range. The map was created using the open-source software Quantum GIS 3.10 with topographic databases ASTER GDEM V2 released by NASA and METI (downloadable from https://asterweb.jpl.nasa.gov), and GADM 2.8 released by Global Administrative Areas (downloadable from http://gadm.org/).

TABLE 1 Sampling information and genetic diversity for *Satsuma batanica* species complex

	Location	Code	N(d)	Coordinates (WGS84)	Alt. (m)	Group	Haplotype (no.)	Nh	S	h	π	T-D	F-Fs
1	Basimo Bridge, Sisigu, Pingtung	B	7 (0)	22.21343, 120.76400	116	6	H1(3), H2(1), H3(1), H4(1), H72(1)	5	32	0.857 ± 0.137	3.944 ± 2.274	0.453	2.396
2	Mt. North Lilongshan, Pingtung	BL	3 (3)	22.19678, 120.72712	320	5	H5(2), H45(1)	2	16	0.667 ± 0.314	2.01 ± 2.323	0	4.289
3	Batan Island, Batanes, Philippines[a]	BT	4 (0)	20.41189, 121.95581		2	H6(4)	1	0	0 ± 0	0 ± 0	0	N.A.
4	Cikong Waterfall, Manjhou, Pingtung	CK	10 (0)	22.02825, 120.79967	227	3	H7(3), H8(3), H9(2), H10(1), H11(1)	5	6	0.844 ± 0.08	0.450 ± 0.030	0.371	−0.274
5	Mt. Chiniuling, Hengchun, Pingtung	CN	15 (0)	21.99452, 120.75547	33	3	H12(10), H13(2), H14(2), H15(1)	4	22	0.552 ± 0.137	1.566 ± 0.860	−0.734	4.981
6	Mt. Dajianshan, Hengchun, Pingtung	D	7 (0)	21.95986, 120.79745	180	3	H16(1), H17(1), H18(5)	3	6	0.524 ± 0.209	0.371 ± 0.270	−1.129	1.222
7	Damei uphill, Mudan, Pingtung	DMd	14 (14)	22.14080, 120.75335	203	1	H10(3), H19(4), H20(1), H21(1), H22(2), H37(2), H78(1)	7	14	0.879 ± 0.058	1.519 ± 0.840	1.915	1.263

a Sequence retrieved from GenBank (Accession number JQ582280–JQ582283; Batomalaque et al., 2013).

TABLE 1 Sampling information and genetic diversity for *Satsuma batanica* species complex (*cont.*)

	Location	Code	N(d)	Coordinates (WGS84)	Alt. (m)	Group	Haplotype (no.)	Nh	S	h	π	T-D	F-Fs
8	Damei foothill, Mudan, Pingtung	DMs	13 (0)	22.12041, 120.74789	118	1	H10(3), H19(4), H21(3), H22(1), H23(1), H37(1)	6	21	0.846 ± 0.065	1.794 ± 0.987	0.449	2.536
9	Mt. Dashanmushan, Hengchun, Pingtung	DS	2 (0)	21.95666, 120.77258	75	–	H24(1), H25(1)	2	5	1.0 ± 0.5	0.916 ± 1.003	N.A.	N.A.
10	Dawu forest road, Dawu, Taidung	DW	3 (0)	22.36185, 120.86837	106	6	H26(1), H27(2)	2	1	0.667 ± 0.314	0.123 ± 0.153	0	0.201
11	Green Island, Taidung	G	12 (0)	22.66380, 121.47898	120	2	H6(12)	1	0	0 ± 0	0 ± 0	0	N.A.
12	Gankou, Manjhou, Pingtung	GK	10 (0)	21.98933, 120.84292	16	1	H10(3), H25(1), H28(1), H29(1), H30(1), H72(1), H99(2)	7	26	0.911 ± 0.077	2.135 ± 1.196	−0.064	0.646
13	Banana Bay, Hengchun, Pingtung	H	13 (0)	21.92871, 120.82871	6	7	H31(2), H32(7), H33(1), H34(1), H35(1), H36(1)	6	6	0.718 ± 0.128	0.202 ± 0.158	**−1.685***	**−2.98***
14	Heren, Shoulin, Huanlien	HR	7 (0)	24.24866, 121.71371	40	1	H37(4), H38(3)	2	10	0.571 ± 0.12	1.328 ± 0.811	2.146	6.638
15	Houwan, Checheng, Hengchun, Pingtung	HW	15 (9)	22.03521, 120.69223	60	3	H39(1), H40(1), H41(1), H42(12)	4	6	0.371 ± 0.153	0.155 ± 0.13	**−1.983***	−0.825
16	Ima Forest Road, Jialan, Taidung	JL	13 (0)	22.59640, 120.97095	91	6	H43(13)	1	0	0 ± 0	0 ± 0	0	N.A.

TABLE 1 Sampling information and genetic diversity for *Satsuma batanica* species complex (*cont.*)

	Location	Code	N(d)	Coordinates (WGS84)	Alt. (m)	Group	Haplotype (no.)	Nh	S	h	π	T-D	F-Fs
17	Jhiben, Beinan, Taidung	JP	1 (0)	22.68767, 120.99310	151	–	H27(1)	1	0	1 ± 0	0 ± 0	N.A.	N.A.
18	Mt. Guanshan, Hengchun, Pingtung	K	13 (0)	21.96512, 120.71923	127	4	H44(1), H45(8), H46(1), H47(2), H64(1)	5	8	0.628 ± 0.143	0.388 ± 0.259	−0.984	−0.159
19	Mt. Gueishan, Checheng, Pingtung	KS	10 (10)	22.04978, 120.70400	30	3	H17(1), H18(1), H42(1), H48(3), H49(4)	5	5	0.8 ± 0.1	0.354 ± 0.247	0.175	−0.787
20	Lanyu (Orchid) Island, Taidung	L	13 (0)	22.01213, 121.56857	43	2	H6(8), H50(1), H51(1), H52(2), H53(1)	5	16	0.628 ± 0.143	1.386 ± 0.777	0.249	2.762
21	Longkeng, Hengchun, Pingtung	LK	10 (0)	21.90219, 120.85617	35	5	H52(1), H54(6), H55(1), H56(1), H57(1)	5	4	0.667 ± 0.163	0.184 ± 0.152	−1.245	**−2.377***
22	Mt. Lilongshan, Pingtung	LL	14 (14)	22.15988, 120.69855	16	8	H58(3), H59(1), H60(7), H61(3)	4	6	0.703 ± 0.095	0.288 ± 0.204	−0.704	0.514
23	River Lanrensi, Manjhou, Pingtung	LR	3 (0)	22.04869, 120.85669	88	5	H80(3)	1	0	0 ± 0	0 ± 0	0	N.A.
24	Pool Longluantan, Hengchun, Pingtung	LT	6 (0)	21.97582, 120.73815	30	4	H2(1), H62(2), H63(1), H64(2)	4	5	0.867 ± 0.129	0.509 ± 0.36	0.878	−0.071

TABLE 1 Sampling information and genetic diversity for *Satsuma batanica* species complex (*cont.*)

	Location	Code	N(d)	Coordinates (WGS84)	Alt. (m)	Group	Haplotype (no.)	Nh	S	h	π	T-D	F-Fs
25	Moubitou, Hengchun, Pingtung	M	16 (0)	21.92723, 120.73714	42	4	H45(1), H65(3), H66(3), H67(1), H68(1), H69(4), H70(1), H71(1), H110(1)	9	26	0.9 ± 0.05	1.798 ± 0.973	−0.197	0.349
26	Mudan, Pingtu	MD	16 (0)	22.13903, 120.80380	190	1	H72(1), H73(1), H74(1), H75(6), H76(2), H77(1), H78(1), H81(1), H99(2)	9	19	0.858 ± 0.077	1.014 ± 0.575	−0.677	−0.998
27	Manjhou, Pingtung	MT	8 (0)	22.01788, 120.84311	30	1	H79(4), H80(3), H81(1)	3	18	0.679 ± 0.122	2.39 ± 1.373	1.96	6.4
28	Mt. Nanrenshan, Manjhou, Pingtung	NR	3 (0)	22.08450, 120.83525	149	2	H72(1), H82(1), H83(1)	3	2	1 ± 0.272	0.253 ± 0.258	0	−1.216
29	Kayofong Waterfall, Shihtze, Pingtung	NS	14 (4)	22.29648, 120.70041	278	5	H84(6), H85(1), H86(7),	3	2	0.604 ± 0.076	0.129 ± 0.116	0.226	0.086
30	Nantien, Daren, Taidung	NT	11 (0)	22.26864, 120.88530	192	1	H87(7), H88(1), H89(1), H90(2)	4	5	0.6 ± 0.154	0.264 ± 0.196	−0.812	−0.11
31	Paoli Experimental Forest, Checheng, Pingtung	P	11 (7)	22.07142, 120.76131	95	1	H8(1), H78(1), H91(1), H92(2), H93(1), H94(1), H95(1), H99(3)	8	27	0.927 ± 0.067	2.324 ± 1.282	0.155	0.145

TABLE 1 Sampling information and genetic diversity for *Satsuma batanica* species complex (*cont.*)

	Location	Code	N(d)	Coordinates (WGS84)	Alt. (m)	Group	Haplotype (no.)	Nh	S	h	π	T-D	F-Fs
32	East of Paoli Experimental Forest, Checheng, Pingtung	PE	12 (1)	22.07417, 120.79228	282	1	H42(1), H78(5), H96(2), H97(1), H98(1), H99(1), H78(1), H100(1)	7	15	0.833 ± 0.1	1.273 ± 0.725	0.67	0.337
33	Sheding, Hengchun, Pingtung	S	14 (0)	21.96647, 120.81590	273	1	H10(1), H25(1), H101(1), H102(1), H103(5), H104(2), H105(1), H106(1), H107(1)	9	37	0.879 ± 0.079	2.701 ± 1.444	−0.318	0.765
34	Shihai, Hotspring, Mudan, Pingtung	SH	2 (0)	22.19849, 120.89122	28	-	H108(1), H109(1)	2	5	1 ± 0.5	0.915 ± 1.001	N.A.	N.A.
35	Mt. Shoushan, Kaohsiung	SS	3 (0)	22.63582, 120.27735	62	4	H45(1), H110(2)	2	1	0.667 ± 0.314	0.127 ± 0.156	0	0.201
36	Shimen Historic Battlefield, Mudan, Pingtung	ST	12 (12)	22.11202, 120.76128	78	1	H111(2), H112(1), H113(2), H114(2), H115(3), H116(1), H117(1)	7	10	0.909 ± 0.056	0.597 ± 0.372	−0.406	−1.377
37	Shihtze, Pingtung	SZ	6 (6)	22.23742, 120.70167	81	5	H118(3), H119(1), H120(2)	3	17	0.733 ± 0.155	1.634 ± 1.014	−0.76	3.637
38	Caopu, Shihtze, Pingtung	TP	8 (0)	22.23494, 120.80365	254	6	H1(2), H72(4), H121(1), H122(1)	4	21	0.75 ± 0.139	2.944 ± 1.676	1.662	4.415

TABLE 1 Sampling information and genetic diversity for *Satsuma batanica* species complex (*cont.*)

	Location	Code	N(d)	Coordinates (WGS84)	Alt. (m)	Group	Haplotype (no.)	Nh	S	h	π	T-D	F-Fs
39	Wanliton, Hengchun, Pingtung	W	13 (0)	22.00370, 120.69674	20	3	H123(2), H124(1), H125(1), H126(7), H127(2)	5	8	0.705 ± 0.122	0.48 ± 0.308	−0.213	0.421
40	Shuanliou, Shihtze, Pingtung	SL		22.21760, 120.79578	180								

Abbreviations and symbols: F-Fs, Fu's Fs test; Group, groups determined by Geneland; h, haplotype diversity (mean ± sd); N.A., calculation cannot be performed; N(d), number of individuals analysed, number of dextral individuals are in parentheses; Nh, number of haplotype; π, nucleotide diversity (mean±sd of Tamura and Nei distance, in percentage); S, number of polymorphic sites; T-D, Tajima D test; Significant values ($P < 0.05$) of Tajima D test and Fu's Fs test are in bold with an asterisk.

longkiauwensis Wu et al., 2007 and *S. succincta* (Adams, 1866) were used as outgroups for the analyses. The two species are among the closest phylogenetically related species on the tree constructed by Hoso et al. (2010).

The nucleotide composition, number of haplotypes (Nh), number of polymorphic sites (S), haplotype diversity (h), and nucleotide diversity (π) were calculated for each population using the software Arlequin ver. 3.5.2.2 (Excoffier et al., 2005). A phylogenetic network of haplotypes was constructed using a median-joining network in POPART v1.7 (Leigh & Bryant, 2015) to evaluate the intraspecific evolutionary relationships among the haplotypes of the *S. batanica* group.

Ancestral state reconstruction

The ancestral states of the coiling directions on the phylogenetic tree were reconstructed using the phytools package in R (R Core Team, 2018; Paradis & Schliep 2019). The coiling directions were recorded for each haplotype. The dataset was analysed using models of continuous-time Markov chain process (extended Mk models) for intraspecific polymorphism, taking into account the co-occurrence of the two directions in the same haplotype. Three models, equal rates for all permitted transitions (ER), all-rates-different for permitted transitions model (ARD), and symmetric backwards and forward rates for all permitted transitions model (SYM), were fitted to analyse the evolution of the two coiling directions. The character's evolution direction was considered to be ordered, as the transition from one coiling to another is expected to pass through a polymorphic stage for each haplotype. The AIC criterion was used to select the best-fitting model. The stochastic character mapping (Huelsenbeck et al., 2003) was performed based on the ML tree. The number of simulations was set to 1,000.

Population demographics

The Fu's Fs neutrality index tests for the hypothesis of selective neutrality and population equilibrium and is more powerful when the sample size is small (Ramírez-Soriano et al., 2008). Data from three populations with fewer than three individuals were excluded from the analyses. The indices were calculated, and significance levels were tested by generating 10,000 simulated samples using Arlequin (Excoffier et al., 2005).

To infer signatures of historical demographic history, the analysis involves examining a mismatch distribution, which represents the distribution of pairwise nucleotide differences between haplotypes. This analysis is conducted using the software Arlequin (Excoffier et al., 2005). The difference between the estimated and observed sum of square deviations (SSD) of mismatch distributions was tested using a goodness-of-fit test with 10,000 simulated replicates.

Historical demographics and divergence time were investigated using the Bayesian skyline plot (BSP) method implemented in BEAST ver. 2.6.7 (Bouckaert et al., 2014). A HKY+Γ model for mutation was chosen for ingroup sequences using Model Finder implemented in IQtree (Nguyen et al., 2015). The Markov Chain Monte Carlo (MCMC) analysis was conducted with 150,000,000 iterations, sampling every 20,000 steps using the Coalescent Bayesian Skyline prior. The

first 25% of iterations were discarded as burn-in. The convergence was assessed using Tracer 1.7 (Rambaut et al., 2018), as previously described. The skyline plot, which shows the median value and the upper and lower bounds of the 95% highest posterior density interval of effective population sizes, was generated by Tracer. The lineage through time (LTT) plot was also analysed using Tracer. The time since the expansion event was estimated based on the limestone at Kuanshan, the hilltop of the southern segment of West Hengchun Hill. The reef fossils were estimated to have formed around 120–130 KYA (Shih et al., 1989), which corresponds to the Alpine Riss-Würm interglacial stage. The calibration point was set at the common ancestor of individuals collected from populations K, M, and LT, indicating a monophyletic group on the phylogenetic trees. A log-normal distribution was used with a mean of 109 KYA, corresponding to the peak of MIS 5d, and a standard deviation of 0.11 (95% highest posterior density (HPD) = 94.4, 130 KYA).

Population structure

The spatial Bayesian clustering methods implemented in Geneland v.4.0.8 (Guillot et al., 2005) were utilized to identify the most probable spatial clusters. The uncorrelated allele frequency model and spatial model were chosen. The maximum rate of the Poisson process was set to the number of sequences, with the uncertainty of coordinates set to 0. The population number was evaluated for k values ranging from 2 to 15. The MCMC simulations were conducted using 1 million iterations, with a burn-in of 500. Ten runs were conducted to assess the stability of the clustering. The genetic cluster with the highest log posterior probability after the burn-in was selected for further analysis.

The genetic differentiation and gene flow among populations were estimated using the Φ_{ST} index and the parameter Nm (equal to $(1\text{-}F_{ST})/2F_{ST}$ for haploid data), as implemented in Arlequin. One-way analysis of molecular variance (AMOVA; Excoffier et al., 1992) was conducted to assess the genetic differentiation among populations. Additional two-way AMOVAs were performed to examine two specific hypotheses: grouping by chirality and grouping by Geneland. Fixation indices (Φ) were computed using the TN93 model (Tamura & Nei, 1993) with gamma correction. The distance takes into account nucleotide frequency and is similar to the previously selected HKY model. The number of permutations for all AMOVA was 10,000. The pairwise Φ_{ST} values were used to construct a population network using SplitsTree v4.14.8 (Huson & Bryant, 2006) through the neighbour-net method.

A Mantel test was conducted to test the hypothesis of isolation by distance (IBD), which examines the presence of a positive correlation between a matrix of genetic differentiation index among populations (Φ_{ST}) and geographic distances. The test was conducted on a dataset containing 36 populations for Arlequin analyses. The second dataset was analysed for IBD by excluding three insular populations (L, G, and BT) and two geographically distant but not genetically unique populations (HR and SS), which may have been recently colonised by long-distance dispersal, as suggested by the phylogenetic trees. A Mantel test was conducted using PAST 4.14 (Hammer et al., 2001).

Results

Sampling and molecular diversity

We obtained 367 sequences from 39 locations, as shown in table 1, which also includes the four GenBank sequences from Batan Island. Among these, 28 locations had all sinistral individuals, six had all dextral individuals, and five had mixed chirality. Of the 127 different haplotypes identified from the COI sequences (GenBank Accession numbers PQ248259–PQ248385), 103 of them were private haplotypes found in only one sampling location. The nucleotide frequencies in the aligned COI gene fragment (551 bp) were as follows: A, 24.5%; C, 16%; G, 19%; T, 40.5%, resulting in a 35% GC content. The TN93 distances between the haplotypes ranged from 0.18% to 11.13%, with an average of 3.57% ± 1.76%. Among the 36 sampling populations with more than two samples, the intra-population genetic variations in haplotype number (Nh) ranged from 1 to 9, with an average of 4.5. The haplotype diversity (h) ranged from 0.0 to 1.0, with an average of 0.66 (table 1). The genetic variations in nucleotide diversity (π) ranged from 0 to 3.94%, with an average of 1.05%. The top three highest nucleotide diversities were found at Basimo Bridge (B), Mt. North Lilongshan (BL), and Caopu (TP). All three locations are situated on the northern edge of the Peninsula along the River Fonggang.

Phylogenetic analyses

The best-fit model for the dataset of ingroup sequences and the two outgroups was determined to be K3Pu+Γ for ML analysis in IQtree and HKY+Γ for BI analysis in MrBayes. The best-fit model for the dataset containing only ingroup sequences was determined to be HKY+Γ. The BI and ML trees exhibit similar topologies in the middle and at the root. Both the BI and ML trees indicate that clade XIV (H1, H4, H121, originating from B and TP) is positioned near the root of the trees (fig. 2). Together with the subsequent close clade XIII (H26, H27, and H43, originating from Taidung), it exhibited a more distant relationship from the other haplotypes. The branches in the middle of the trees are well-supported and can be identified as 14 clades. Most clades consist of samples primarily collected from a single location (e.g., clades II, V, VI, IX, X, XI) or from nearby areas (e.g., clades I, III, VII, VIII, XIII, XIV). Although the clades do not distinctly correspond to geographic populations, the phylogenetic trees still tend to exhibit geographic structures. Incidentally, three locations (SS, HR, and BT) are geographically distant from the primary distribution of the species, which is the Hengchun Peninsula. The three SS samples share the haplotype with samples collected from K, M, and BL in clade VII. The HR samples share one haplotype with DMd and DMS in clade I and have a unique haplotype in clade III. The BT samples have only one haplotype (H6) shared with L and G. These haplotypes in the three populations may be the result of recent long-distance dispersal.

Among the 127 haplotypes, 25 consisted entirely of dextral individuals, 12 were mixed, and 90 were composed entirely of sinistral individuals. Among the 14 clades, only clade II (LL) consisted entirely of dextral individuals. Five clades (I, III, VI, VII, and VIII) were a combination of both coiling directions, while the remaining eight clades were exclusively sinistral

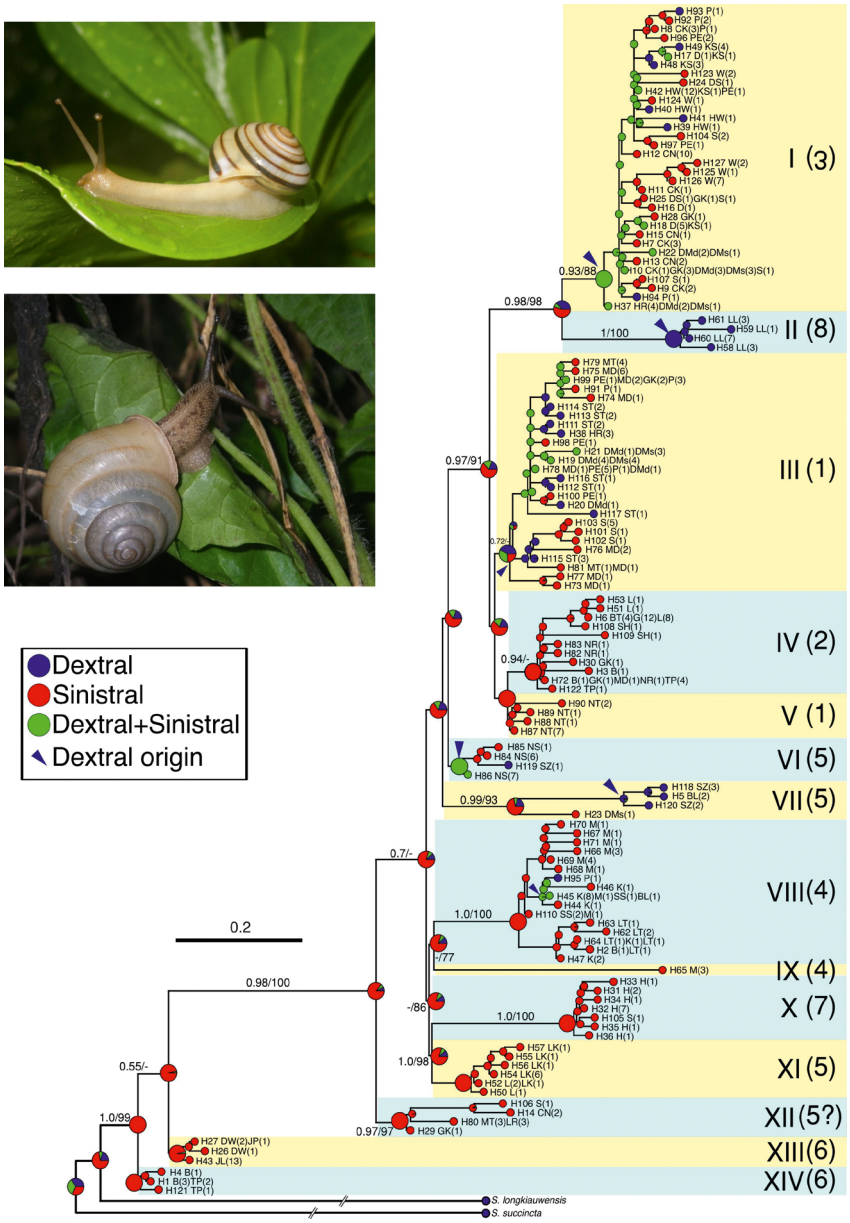


FIGURE 2 Phylogenetic relationships among the haplotypes of the COI gene of the *Satsuma batanica* species group. The tree is based on the maximum likelihood tree with ancestral states of chirality mapped at the nodes. Numbers beside branches indicate branch support based on posterior probability for BI tree (left) and ultrafast bootstrapping for ML tree (right). Only the branch supports for the major clades are shown. The pie charts at some internal nodes are enlarged. Arrows are the possible origin of reverse chirality counted only once in each clades. Phylogenetic clades are labelled as Roman numerals; Geneland groups are labelled as Arabic numerals in parentheses.

individuals (fig. 2). Among the five populations (HW, HR, NS, P, and PE) that coexist with both sinistral and dextral individuals, the haplotypes of HW and NS were each grouped in phylogenetic clades I and VI, respectively. The haplotypes of PE were distributed across clades I and III, while the haplotypes of P were mainly found in clades I and III, with one individual in clade VIII clustering with samples from K. HR shares one haplotype with DMS and DMd.

For the ancestral state reconstruction, the best-fit model among the three models was the ARD model with an order. The phylogenetic tree (fig. 2) indicates that the most recent common ancestor (MRCA) of the *S. batanica* species group was sinistral. The ancestors of clades I, III, and VI have a higher probability (greater than 0.5) of being polymorphic. The ancestor of clade II was dextral, while the ancestors of the other ten clades were sinistral. Due to the limited support for terminal branches within clades, evolutionary events in a clade were counted conservatively only once. Subsequently, the transition from sinistral to dextral morph occurred at least six times in six of the 14 clades: clades I, II, III, VI, VII, and VIII. Additional origins of dextral morph and potential reversals may have occurred within clades, but these were difficult to confidently assess, particularly those within the two large polymorphic clades I and II. Therefore, these were omitted here.

The median-joining network (fig. 3), similar to the BI and ML trees (fig. 2, supplementary figs. S1–S2), separated the haplotypes into the same 14 clades (framed and highlighted in yellow). The unresolved and missing haplotypes that diverged into clades VI–XII without a clear branching pattern exhibited similar polytomous clades in both the BI and ML trees. The unresolved area may be a centre of origin, representing the most recent common ancestor in the phylogenetic trees. The clades I–V formed a monophyletic group, as indicated in the two phylogenetic trees. The three polytomous clades in the BI tree (clades V, VI, XIV) showed more pronounced clustering in the network compared to the BI tree and were similar to the ML tree.

Population demographics and divergence times

The estimated values of Fu's Fs and Tajima's D for the overall populations were found to be −23.72 ($p < 0.05$) and −0.73 ($p > 0.05$), respectively. Estimates for each population were significantly negative at populations H and LK according to Fu's Fs test, and at populations H and HW according to Tajima's D (table 1). The negative parameters indicate that these populations have undergone natural selection and a recent population expansion. The overall mismatch distribution (fig. 4A) fit a unimodal distribution. The SSD value (0.0018) did not significantly deviate from a unimodal distribution, indicating that these populations have experienced a demographic expansion.

The estimated median age of the MRCA of the *S. batanica* species group, as determined by BEAST, is more recent than 615 KYA (fig. 4). The Bayesian Skyline plot (fig. 4B) illustrates the changes in effective population size over time for overall populations. The plot depicted a prolonged period of stable population size since the emergence of the MRCA of the *S. batanica*

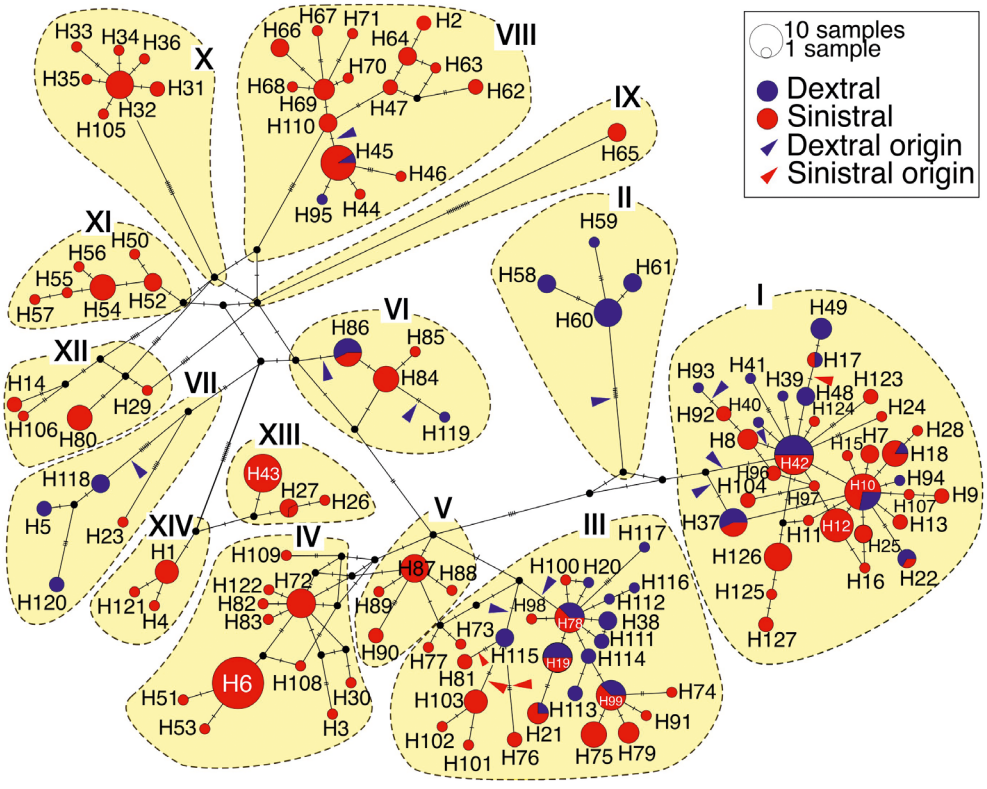


FIGURE 3 Median-joining haplotype network of 128 haplotypes. The size of the circles is proportional to the frequency of each haplotype. The two colours represent the percentage of chirality. The red is sinistral shell and the blue is dextral shell. The hatch marks represent the mutational steps between haplotypes. Small black circles indicate missing haplotypes. Arrows are the possible origin of reverse chirality.

species group, followed by a recent and brief demographic expansion estimated to have commenced around 50 KYA. The major clades observed in phylogenetic trees and network diverged approximately after 440 KYA (fig. 4C). The most recent divergent events within clades and the expansion of the population size occurred after 100 KYA. These results were also confirmed by the two waves of mismatch distribution (fig. 4A), although they were not statistically significant. The CO1 gene exhibited clocklike behaviour, as the value of ucld.stdev (0.55) was smaller than 1.0 (Drummond et al., 2006). The average substitution rate calculated by BEAST was 0.0496 ± 0.0168 (mean ± sd) per site per million years for CO1. The average molecular clock rate for CO1 markers was faster than 9.92% per million years, given that the calibrated date of 109 KYA, is considered the earliest possible colonisation date.

Population structure

All ten runs of the Bayesian clustering by Geneland identified the same optimal number of clusters (K = 8). The cluster

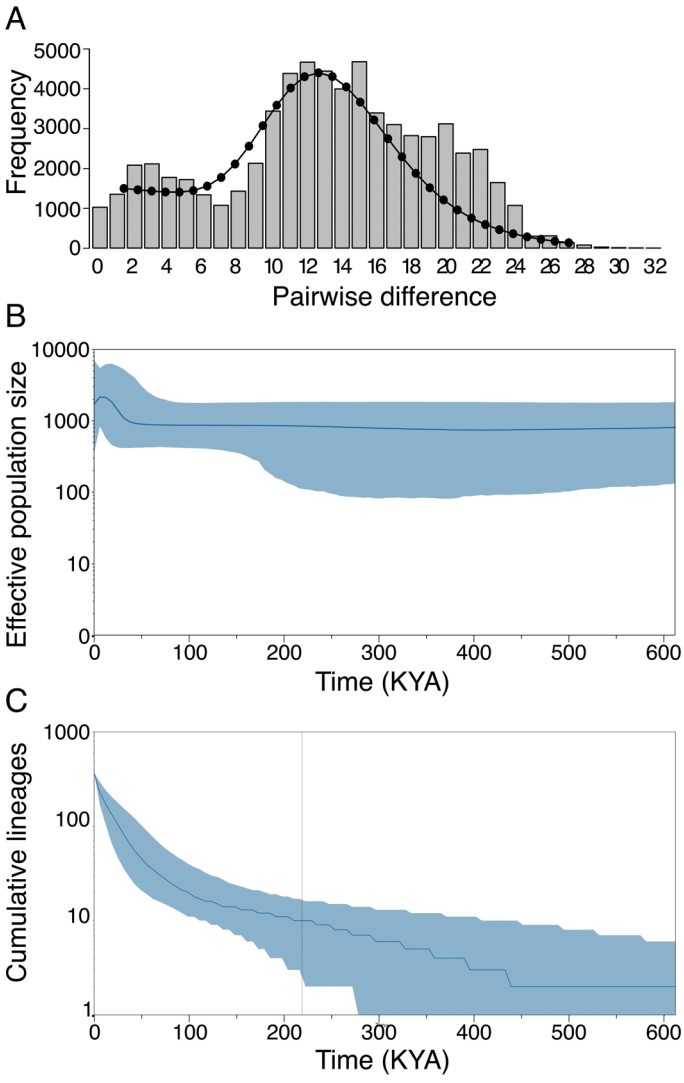


FIGURE 4 Mismatch distribution and Bayesian skyline plot based on the COI gene of *Satsuma batanica*. (A) Mismatch distributions showing the observed pairwise differences (grey bars) and the expected expansion models (black lines). (B) Bayesian skyline plot. (C) Lineage through time (LTT) plot.

with the highest log posterior probability (–5287) was chosen for subsequent analyses (fig. 4). The clustering of the second highest probability (–5499) resulted in the population NT being grouped in group 2 instead of group 1. A similar uncertainty was also observed in the MJ network at NT (fig. 3). The cluster containing haplotypes from NT, which is equivalent to clade V, was positioned between clade

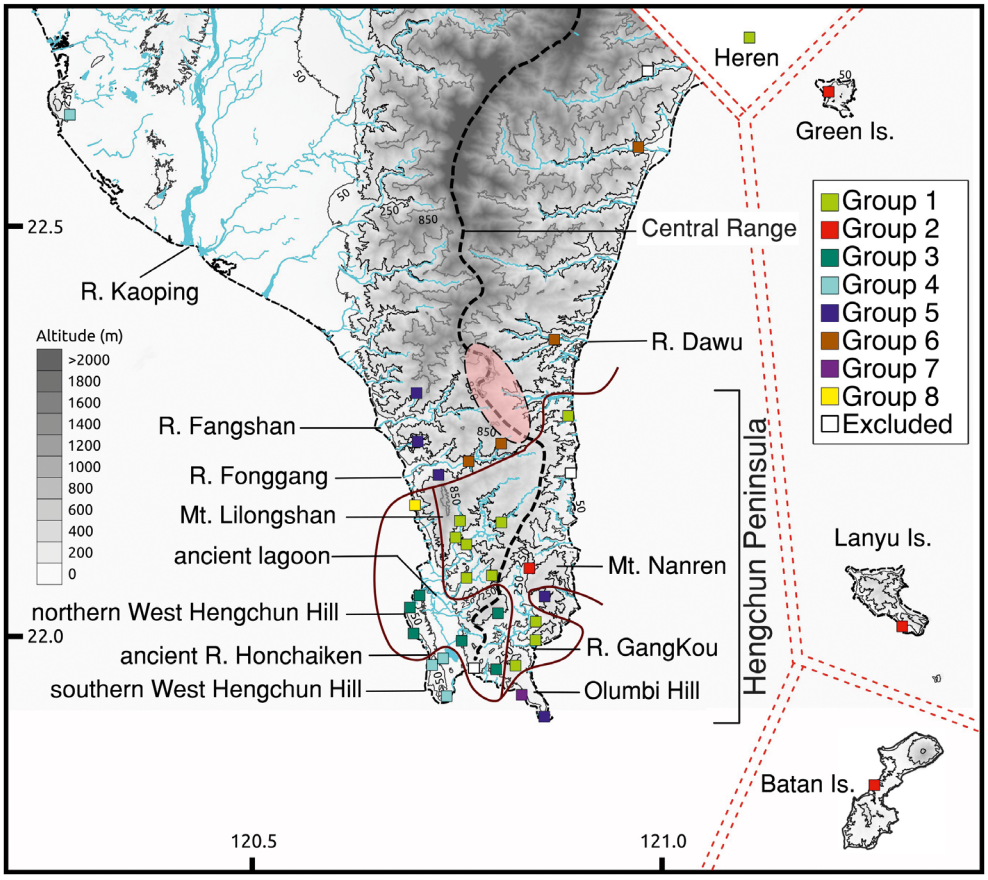


FIGURE 5 Spatial genetic clustering defined by GENELAND. The possible origin area is coloured pale red. Brown lines border the locations of group (1, 2) on east and (3, 8) on west in Hengchun Peninsula.

III (comprising the majority of group 1) and clade IV (comprising the majority of group 2). Most determined clusters followed the isolation-by-distance model and were clustered with nearby populations. The exceptions were in group 5, which included populations from the northwest (NS, SZ, BL), eastern (LR), and southeast (LK) of the Hengchun Peninsula. The genetic differentiation between populations was estimated using two indicators, Φ_{ST} and Nm (supplementary tables S1–S2). Most of the Φ_{ST} values were significantly different between populations. Compared to the clustering of Geneland, the tests for Φ_{ST} values tend to show greater differentiation. For example, MT and MD were excluded from the other members in the Geneland group 1 (DMd, DMS, GK, HR, P, PE, and S).

One-way AMOVA based on Tamura and Nei distances indicated significant differentiation among the 36 analysed populations (table 2, Φ_{ST} = 0.70, $p < 0.05$).

TABLE 2 Table of analysis of molecular variance (AMOVA) along with fixation indices for population genetic structure of *Satsuma batanica* with A. not grouped, B. grouped by chirality, C. grouped by Geneland result (k = 8).

Not grouped

Source of variation	d.f.	Sum of squares	Variance components	Variance (%)
Among populations	35	2412.87	6.60*	69.61
Within populations	326	939.48	2.88	30.39
Total	361	3352.36	9.48	

Fixation Index: Φ_{ST} = 0.696

Grouped by chirality

Source of variation	d.f.	Sum of squares	Variance components	Variance (%)
Among groups	1	73.16	0.18	2.55
Among populations within groups	39	1661.51	4.62 *	65.85
Within populations	321	711.82	2.22 *	31.59
Total	361	2446.50	7.02	

Fixation Indices: Φ_{SC} = 0.676, Φ_{ST} = 0.684, Φ_{CT} = 0.026

Grouped by Geneland

Source of variation	d.f.	Sum of squares	Variance components	Variance (%)
Among groups	7	1334.81	4.22 *	55.17
Among populations within groups	28	384.64	1.20 *	15.69
Within populations	326	727.05	2.23 *	29.14
Total	361	2446.50	7.65	

Fixation Indices: Φ_{SC} = 0.350, Φ_{ST} = 0.709, Φ_{CT} = 0.552

Abbreviations and symbols: Φ_{CT}: genetic differentiation between groups relative to total; Φ_{SC}: genetic differentiation between subpopulations relative to group; Φ_{ST}: genetic differentiation between subpopulations relative to total; *, significant ($p < 0.05$) of permutation test.

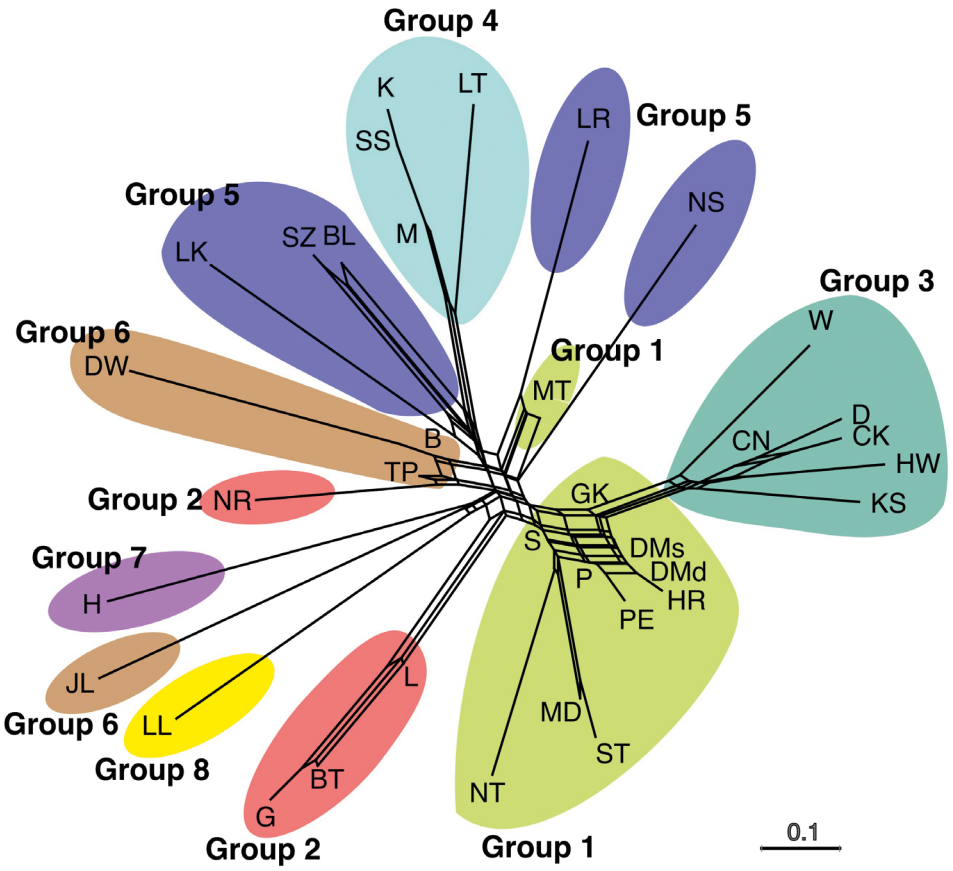


FIGURE 6 Population network based on pairwise Φ_{ST} values between 36 populations of *Satsuma batanica* constructed by the neighbour-net method

When testing the alternative hypotheses by grouping the same coiling direction, the variance among the two groups is not significant (table 2, Φ_{CT} = 0.026), as anticipated based on the result of the phylogenetic tree. When testing the alternative hypotheses by applying the grouping determined by Geneland, the variance among the eight groups explains 55.1% of the total variance and is statistically significant (table 2, Φ_{CT} = 0.552, $p < 0.05$). The Φ_{CT} value is high relative to Φ_{ST} (0.706), indicating the presence of substantial population genetic structure at the group level.

The neighbour-net network for populations (fig. 6) based on the Φ_{ST} between populations (supplementary table S1) exhibited a similar pattern to the grouping identified by Geneland. The exceptions were observed at MT of group 1, NR of group 2, LR and NS of group 5, and JL of group 6. In other words, the neighbour-net method identified more clusters than Geneland, which is similar to the grouping shown in the phylogenetic trees and MJ networks (figs. 2–3, supplementary fig. S3).

The test for isolation by distance (IBD) was conducted for 36 populations, and it revealed a non-significant correlation

between geographic and genetic distances ($r = 0.054$, $p > 0.05$). The test for the reduced dataset, which excluded five populations, revealed a significant correlation ($r = 0.419$, $p < 0.05$), indicating that an isolation by distance model occurred in the Peninsula.

Discussion

No evidence for single-gene speciation

The present study offers insight into the impact of chirality on the genetic divergence among land snails of the *S. batanica* species group across populations spanning its entire geographic range. Most studies that supported single-gene speciation by chirality using phylogenetics were conducted among species within a genus, with only one or a limited number of individuals analysed for each species (Ueshima & Asami, 2003; Hoso et al., 2010; Fehér et al., 2013). The frequent reversals from sinistral to dextral morph, and vice versa, though less common, on the phylogenetic trees observed in this study can be interpreted as being caused by a single-gene and biallelic controlled mutation of the chirality, genetic introgression, and incomplete lineage sorting of an opposite coiling morph (Maddison & Knowles, 2006; Davison et al., 2016). Each reversal in coiling direction is less likely to indicate a potential mutation in the opposite direction. Several molecules, such as the signalling molecule Nodal (Grande & Patel, 2009) and diaphanous-related Formin homology proteins in freshwater snails, are thought to be associated with the asymmetry of snails (Davison et al., 2016). However, these genetic loci are conserved and associated with clades in deep phylogeny above the family level (Grande & Patel, 2009; Davison et al., 2016) or above the species level (Ueshima & Asami, 2003; Hoso et al., 2010). They may not be sufficient to explain the frequent intraspecific mutations (Davison, 2020). The phylogeny of the two genera, *Euhadra* and *Partula*, with chiral polymorphism based on one of the candidate genes, dia, did not support the association between chirality and the gene (Davison et al., 2016). The chiral variations in the *S. batanica* species group may involve additional pathways or gene variants, as suggested by Davison et al. (2016) for *Euhadra* and *Partula*.

The genetic introgression and incomplete lineage sorting should be considered as factors resulting in the frequent chiral reversal in *S. batanica*. Genetic introgression, also known as introgressive hybridisation, refers to the transfer of alleles from one taxon into the gene pool of another taxon through hybridisation and backcrossing (Harrison & Larson, 2014). Incomplete lineage sorting describes the random retention of ancestral polymorphisms between taxa, particularly in recently evolved groups (Maddison & Knowles, 2006). Genetic introgression is being increasingly observed in animals and plants (Dowling & Secor, 1997), including several lineages of land snails in the family Camaenidae (Shimizu & Ueshima, 2000; Chiba, 2005; Morii et al., 2015). Distinguishing between chiral introgression, incomplete lineage sorting of chirality, and mitochondrial mutation based on the current mitochondrial phylogeny is challenging. This is because the candidate genes for chirality are maternally expressed, mitochondrial DNA is maternally inherited (Schilthuizen et al., 2005), and the terminal nodes of the phylogenetic

trees still need to be fully resolved with high support. The polymorphic clades and populations display extensive chiral polymorphism and mitochondrial introgression. Consequently, the evolutionary history of chirality remains unclear. Incidentally, our results do not support the existence of a hybrid zone formed by the secondary contact between dextral populations on the northwestern Hengchun Peninsula and sinistral populations. This is because the dextral populations are not monophyletic, indicating that the chiral sympatry is likely caused by stochastic or evolutionary processes rather than a simple biogeographic one. Utilising genotypic markers across the whole genome can help to clarify potential genetic introgression (Richards et al., 2017). The less observed evolution from dextral to sinistral morph may be caused by the more recent (less than 0.6 MYA) evolutionary history of the species group. There is probably insufficient time to accumulate the secondary mutation or genetic introgression from the newly acquired dextral to sinistral morph. Furthermore, reverse evolution within the two large clades I and III may occur more frequently than the current phylogenetic markers can resolve (supplementary figs. S1–S2). Since dextral snails predominate in *Satsuma* (about 83%; Hwang & Wu, 2018), the dextral phenotype may have been favored in the evolutionary history of the genus due to factors involved in the developmental process. These factors range from molecular and cellular to population level, such as physicochemical properties of chiral-related proteins, their expression and regulation, and positive frequency-dependent selection (Hoso et al., 2010; Bershtein et al., 2017; Davison, 2020).

The hypothesis of single-gene speciation based on chiral differences (Orr, 1991; Ueshima & Asami, 2003) is not supported by our results, at least not for this species group. The opposite coiling directions have long been considered a significant factor in reproductive isolation due to the mechanical and behavioural incompatibility between snails with different coiling directions (Orr, 1991; Ueshima & Asami, 2003). This contributes to the speciation of individuals that acquire the newly mutated coiling direction. This aspect is supported by the speciation of the sinistral MRCA of *S. batanica* from its more likely dextral or polymorphic ancestor (fig. 2; Hoso et al., 2010). When examining the populations and haplotypes, the current results do not support reproductive isolation due to the shared haplotype by different chiral morphs (12 out of 127 haplotypes), the coexistence of the two morphs (5 out of 39 locations), and the presence of both chiral morphs in the same phylogenetic clades (5 out of 14 clades). That is, the two chiral morphs are not each monophyletic, and they are neither completely allopatric nor parapatric in their distribution. Regardless of how the reverse coiling gene was introduced into a population, whether through single-gene mutation or genetic introgression via dispersal-hybridisation, the reproductive isolation between the two chiral morphs is incomplete.

To what extent does chirality affect reproductive isolation and, consequently, speciation? The shape of the shell, whether high-spired or low-spired, was considered to have a differentiating effect on the copulation success between snails with different coiling directions (Davison & Mordan, 2007; Johnson, 1982). Copulation experiments on the tree snails *Partula* in

Society Islands with high-conical shells demonstrate that the copulation success for snails with opposed coiling pairs is only 20% as frequent as those with the same coiling pairs (Johnson, 1982). *Amphidromus*, high-conical tree snails, exhibit frequent mating between chiral morphs (Schilthuizen et al., 2007). On the contrary, it was previously believed that depressed-conical snails do not copulate between dextral and sinistral individuals because they cannot perform a "shell-mounting" strategy for successful copulation (Asami et al., 1998; Davison & Mordan, 2007). The "single-gene speciation" hypothesis was supported by phylogenetic studies of Japanese *Euhadra* species (Ueshima & Asami, 2003), which suggested that the chiral direction alone may lead to the formation of a new species. A similar inference was also made for the predominantly depressed-conical land snail *Satsuma* (Hoso et al., 2010). However, interchiral copulation between *Euhadra* species was observed directly and confirmed by genomic SNPs and mtDNA characters from a larger number of samples within and between populations (Richards et al., 2017). The multilocus evidence also supports the idea that chirality alone is not sufficient to maintain the distinctiveness of the dextral *Alopia livida* and the sinistral *Alopia straminicollis* (Koch et al., 2017). The previously mentioned single-gene speciation, caused by the physical barrier between individuals of reverse chirality, is once again being questioned in light of recent evidence.

Since chirality alone is not sufficient for genetic divergence and speciation of *Satsuma*, other factors such as restricted gene flow due to geographic isolation, ancient geological history, and ecological and behavioural differentiation, should be considered. These factors result in local adaptation and the local fixation of coiling, as discussed in the next section. Among these, semi-arboreal behaviour may also contribute to the speciation of the *Satsuma batanica* species group. The semi-arboreal behaviour of *S. batanica* is unique in *Satsuma*. All species in the same clade containing *S. batanica* (the clade after the branching of *S. sphaeroconus*) in the phylogenetic tree of Hoso et al. (2010) are fully terrestrial snails. Given that semi-arboreal behaviour is prevalent in the entire *S. batanica* species, we can speculate that this behaviour may have been an ancestral characteristic of the species, emerging around the same time as, or even earlier than, the origin of sinistrality. We do not know how semi-arboreal behaviour affects genetic differentiation within and between populations. It may increase genetic differentiation through sympatric isolation between individuals on different trees, or decrease genetic differentiation by allowing individuals to crawl across tree canopies and overcome geographic barriers. The observation of *Amphidromus* showed that the arboreal snails frequently crawl across trees, and the arboreal behaviour does not seem to play a role in genetic divergence (Schilthuizen et al., 2005). We speculate that semi-arboreal behaviour may increase gene flow at a local scale, either through movement between tree branches or across the ground.

Genetic structure and phylogeographic history

The MRCA of the species group likely originated from the northern part of the Hengchun Peninsula (fig. 5, pink circle), along the ridge of the uplifted landmass at

the southernmost tip of the Central Range after approximately 600 KYA (fig. 4). Based on the phylogenetic trees (fig. 2), the populations of the two basal clades, clades XIII (JL, DW, and JP) and XIV (B and TP), are distributed in the area. Since the primary distribution area of the *S. batanica* species group is on the peninsula, Mt. Lilongshan, the highest, most extensive and earliest uplifted mountain peak on the Peninsula (Kao, 2020), is the best candidate as the origin centre for the biota on the Peninsula. The phylogenetic trees, however, revealed the three populations located on the Mt. Lilongshan: LL in clade II, and DMd and DMS in clades I and III, is located on the terminal branch and diverged relatively late (figs. 2–3). Therefore, it is unlikely that Mt. Lilongshan is the centre of origin for the *S. batanica* species group. Furthermore, as the oldest landmass on the Peninsula, Mt. Lilongshan was sufficiently high and tremendous enough to serve as a geographic barrier, hindering gene flow between populations on its western side (LL) and eastern side (DMd and DMS) during the expansion and diversification of the species.

The current molecular evidence does not support the hypothesis of the origin from Batanes. The biota on the Hengchun Peninsula, Lanyu Island, Green Island, and parts of eastern Taiwan show an affinity with those in the northern Luzon islands of the Philippines. Therefore, their biogeographical zonation was thought to be included with the Philippines (Lin, 1974). Molecular evidence from animals, such as the stick insect *Megacrania tsudai* and the snake genus *Hebius* (Kobayashi et al., 2014; Kaito & Toda, 2016), also supports the hypothesis of a southern origin. The potential dispersal mechanisms for these organisms include rafting by the strong northward paleo-Kuroshio Current and tropical cyclones, which have been prevalent since the early Pliocene (Gallengher et al., 2015; Hwang et al., 2021). However, the present study did not support the northward dispersal, as the haplotypes containing BT, L, and G are located at the terminal branches of the phylogenetic trees (figs. 2–3). The populations on Batan Island and Green Island are more likely to disperse from Lanyu Island because Lanyu Island exhibits higher genetic diversity (Nh = 5, h = 0.63) compared to the two islands (Nh = 1, h = 0). This indicates that Lanyu Island has a longer evolutionary history compared to Batan Island and Green Island, which have experienced relatively recent colonisation events with only one haplotype. The southward dispersal observed in the present land snails coincided with molecular evidence found in weevil and shrew (Esselstyn & Oliveros, 2010; Tseng et al., 2018). Since the southward dispersal is contrary to the dispersal power of oceanic currents and cyclones, it is important to consider dispersal through hitchhiking via humans or birds (Kramarenko, 2014). The "Out of Taiwan" hypothesis suggests that Austronesian people settled in the Batanes from Taiwan more than 4,000 years ago (Bellwood & Dizon, 2005). An alternative study considers that there were extensive and recent trading activities between the two areas 100–3,000 years ago (Loo et al., 2011). The species was likely transported to Batan Island by humans relatively recently, probably no earlier than 4,000 years ago.

The ancient islands hypothesis has been used to explain the high biodiversity

of clausiliid land snails in Taiwan on a large geographical scale by considering the major mountain ranges as islands (Hwang et al., 2022). We present a small-scale example supporting the ancient island hypothesis by considering the uplifted landmasses as islands. Based on the phylogenetic trees, the species first colonised southeastern areas of the Peninsula (clade XII), approximately in the vicinity of present-day Sheding (S, the hilltop of Olumbi Hill) or Mt. Nanren (MT and GK), after the origin of the species 615 KYA. This event corresponds to the formation and subsequent uplift of coral reefs on Olumbi Hill around 500 KYA (Shih et al., 1989). The species then colonised the currently marginal distribution areas, including the foothills of Olumbi Hill (H and LK), the southern West Hengchun Hill (K and M), and the northwestern part of the Peninsula (SZ and NS). Dispersal events may have contributed to the colonisation of these southern areas, as they were still isolated landmasses at that time. The colonisation of the species to the current core distribution areas was the most recent, corresponding to Geneland cluster groups 1 and 2 in the east, and groups 3 and 8 in the west of the Hengchun Peninsula (fig. 5, brown lines). These areas contain both sinistral and dextral morphs and three sympatric locations. The gradual emergence of ancient landmasses above sea level, coupled with the development of drainage basins in the southern part of the Central Range on the Peninsula (Giletycz et al., 2015) may have created additional habitats for biotas. This could have facilitated dispersal and range expansion events among the ancient landmasses. The geological, ecological, and intrinsic factors also play essential roles in the genetic divergence and demographic expansion during this stage. The drier and cooler climate during the last glaciation age (Würm glaciation, 109–14 KYA) than nowadays appears to have had a favourable effect on the survival of *S. batanica*, as evidenced by the effective population size increase during the Last Glaciation Maximum (MIS2, the coldest period). The mature forests on the young landmass and the semi-arboreal behaviour may also contribute to the survival and divergence of this land snail.

Taxonomy

Family Camaenidae Pilsbry, 1895

Genus *Satsuma* A. Adams, 1868

***Satsuma batanica* (Adams & Reeve, 1850)**

(fig. 7)

1850 *Helix batanica* Adams & Reeve, p. 60, pl. 15, fig. 5a–b.

1866 *Helix bacca* Pfeiffer, p. 829, pl. 46, fig. 8. [1865].

1891 *Helix* (*Hadra*) *pancala* Schmacker & Boettger, pp. 161–163, pl. 1, fig. 6, 6a, 6b.

1891 *Helix* (*Hadra*) *pancala* var. *trifasciata* Schmacker & Boettger, pp. 162–163.

1907 *Eulota* (*Euhadra*) *warburgi* Gude, pp. 164–165.

1932 *Coniglobus* (*?*) *batanica boteltobagoensis* Kuroda, p. 9, pl. 1, fig. 6–8.

2021 *Satsuma backeljaui* Thach & Huber in Thach, pp. 98–99, pl. 75, no. 773–774.

2021 *Satsuma abletti* Thach & Huber in Thach, p. 99, pl. 75, no. 776–777.

Material examined. Type material: Helix batanica: Syntype NHMUK 20040592 (3 shells, fig. 7a), type locality: Island of Batan (Bashee group). *Helix bacca*: Lectotype NHMUK 20040577/1 (fig. 7e), paralectotype NHMUK 20040577/2 (1 shell),

type locality: Formosa [Taiwan]. *Helix* (*Hadra*) *pancala*: Lectotype SMF 8812/1 (fig. 7c), paralectotype SMF 8813/5, type locality: Süd Cap von Formosa [South Cap = nowadays Ouluambi and Longkeng, Hengchun, Pingtung]. *Helix* (*Hadra*) *pancala* var. *trifasciata*: Lectotype SMF 8810 (fig. 7d), paralectotype SMF 8811/3, type locality: Süd Cap von Formosa. *Eulota* (*Euhadra*) *warburgi*: Holotype NHMUK 1922.8.29.66 (fig. 7f), Type locality: Dune at Long-Krau, southern Formosa [nowadays the area between Kueishan and Checheng, Pingtung]. *Coniglobus* (*?*) *batanica boteltobagoensis*: Holotype NC H236 (fig. 7b), paratype NC P227, type locality: Lanyu. *Satsuma backeljaui*: Holotype RBINS [register number missing!], paratype MNHN-IM-2000-35977, F. Huber's collection, type locality: Lanyu Island, Taitung County, Taiwan. [types not examined in person, photographs available online at https://science.mnhn.fr/]. *Satsuma abletti*: Holotype NHMUK 20210117, paratype MNHN-IM-2000-35978, F. Huber's collection, type locality: Lanyu Island, Taitung County, Taiwan. [types not examined in person, photographs available online at https://science.mnhn.fr/]. *Non-type specimens*: see table 1.

Remark. The mitochondrial phylogenetics in the present study revealed that the samples of the dextral morph, currently classified as *S. bacca*, and the sinistral morph, currently classified as *S. batanica* ssp., are not each monophyletic. Four out of the six clades containing dextral morphs are a mix of sinistral morphs both phylogenetically and geographically. The two chiral morphs show no signs of being monophyletically diverged and then coming into contact later in the sympatric populations. The dextral species, *S. bacca*, and the three sinistral (sub-)species, *S. batanica batanica*, *S. b. boteltobagoensis*, and *S. b. pancala*, are conchologically and anatomically indistinguishable (Tabe, 1937; Sinagawa, 1979; Chang, 1992; Hwang, 2012; Hsieh et al., 2013). The identification of the four taxa is primarily based on the coiling direction and sizes of the shells, as well as their isolated distributions on different islands. Although direct observation of copulation between the two chiral morphs of the *S. batanica* species group in the field and laboratory has not been reported, the observed inter-chiral matings in *Euhadra* and *Amphidromus* of the same family (Schilthuizen et al., 2007; Richards et al., 2017) suggest that copulation between the two chiral morphs of *S. batanica* is possible. The influence of chirality on the copulation of the *S. batanica* species group is believed to be minimal and is insufficient for maintaining distinct species of the two chiral morphs. The two species, *S. backeljaui* Thach & Huber in Thach, 2021 and *S. abletti* Thach & Huber in Thach, 2021, were recently described from Lanyu based on only scant specimens (Thach, 2021). The descriptions of the two species were based solely on the colour, thickness, and sizes of shells, without taking into account modern biological knowledge, such as polymorphism of colour and banding patterns, and variations among individuals and populations (Páll-Gergely et al., 2020). The two species are not valid because they are within the range of morphological variations of the previously described subspecies, *S. b. boteltobagoensis*. In summary, we recommend that the seven names, of which three are currently considered valid, two were previously

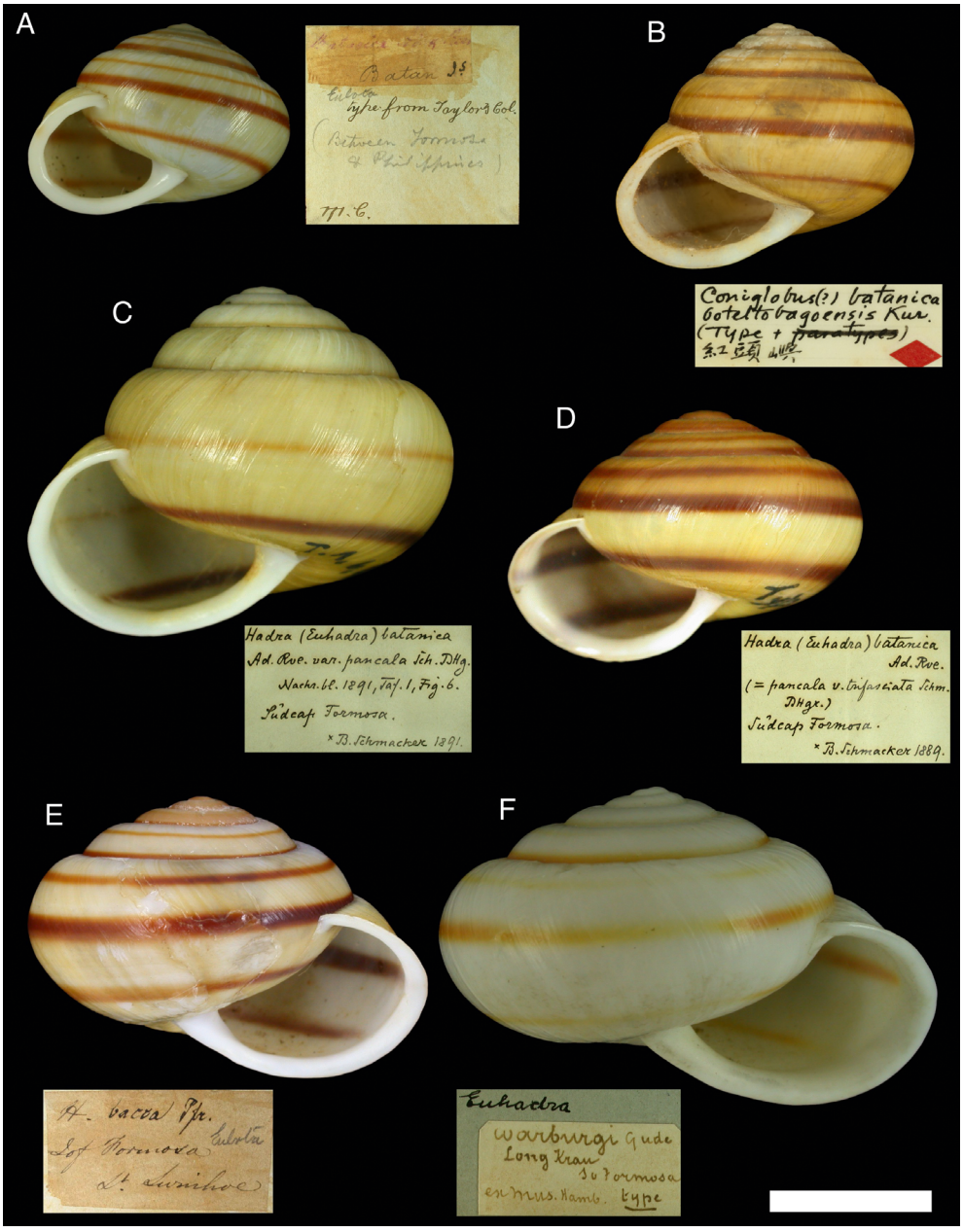


FIGURE 7 Photographs of the type specimens of the taxa currently classified as *Satsuma batanica*. (A) *Satsuma batanica*, syntype NHMUK 20040592. (B) *Coniglobus batanica boteltobagoensis*, holotype NC-H236. (C) *Helix pancala*, lectotype SMF 8812/1. (D) *Helix pancala* var. *trifasciata*, lectotype SMF 8810. (E) *Helix bacca*, lectotype NHMUK 20040577/1. (F) *Eulota warburgi*, holotype NHMUK 1922.8.29.66. Scale = 10 mm.

treated as synonyms, and two are recently described names, should be treated as the same species without any subspecific designation. This recommendation is based on conchological, anatomical, and molecular characters, as well as their geographic distribution (Sinagawa, 1979; Chang, 1992; Hwang, 2012). According to the priority criteria of the ICZN (1999), the name *Satsuma batanica* (Adams & Reeve, 1850) should be used as a valid name. The seven names are synonyms: *Helix bacca* Pfeiffer, 1866 with one previous synonym *Eulota* (*Euhadra*) *warburgi* Gude, 1907, *H. pancala* Schmacker & Boettger, 1891 with one previous synonym *Helix* (*Hadra*) *pancala* var. *trifasciata* Schmacker & Boettger, 1891, *Coniglobus batanica boteltobagoensis* Kuroda, 1932, *S. backeljaui* Thach & Huber in Thach, 2021, and *S. abletti* Thach & Huber in Thach, 2021.

Acknowledgements

We gratefully acknowledge the assistance of Dr Hsueh-Wen Chang and Dr Kuan-Min Chang for their direction and support for the study of land snails. We thank Jin-Yu Fan, Kuo-Chiang Liu, Jin-Kuan Yang, Shin-De Yang, Bing-Lin Shih, Tian-Tsai Chen, Gaus Shiang, Shih-Bo Lee, Zong-Hang Yang, Yang-Wei Wang, Yu-Jie Lin, and Ying-Shuang Lu for their help in our fieldwork. We are grateful to Fred Naggs, Jonathan Ablett, Ronald Janssen, Eike Neubert, Kenji Ohara, and Yoko Otani for their assistance in examining and photographing specimens. We are indebted to the Biodiversity Heritage Library and Páll-Gergely for providing access to rare literature for this work. We thank Chuan-Chin Huang for valuable comments and suggestions on a previous draft of the manuscript. Angus Davison and one other reviewer are gratefully acknowledged for their constructive and detailed comments. We also wish to express our gratitude to the Kenting National Park and the Taiwan Forestry Research Institute of the Council of Agriculture for granting us collection permission in Taiwan.

Supplementary material

Supplementary material is available online at:
https://doi.org/10.6084/m9.figshare.26976883

References

Adams, A. & L. Reeve (1850) Mollusca, Part III. In: Adams, A. (ed) *The Zoology of the Voyage of H.M.S. Samarang; under the Command of Captain Sir Edward Belcher, C.B., F.R.A.S., F.G.S., during the Years 1843–1846*, pp. 1–87. Reeve, Benham & Reeve, London.

Asami, T., Cowie, R.H., & Ohbayashi, K. (1998) Evolution of mirror images by sexually asymmetric mating behavior in hermaphroditic snails. *Am. Sci.*, 152, 225–236.

Azuma, M. (1995) *Colored Illustrations of the Land Snails of Japan*. Hoikusha, Osaka.

Batomalaque, G., Sales, P.R., & Fontanilla, I.K. (2013) DNA barcoding using cytochrome oxidase I (COI) of pulmonate gastropods from Batan Island, Batanes, Philippines. *Asia Life Sci.*, 22, 341–357.

Bellwood, P. & Dizon, E. (2005) The Batanes Archaeological Project and the "Out of

Taiwan" hypothesis for Austronesian dispersal. *J. Austron. Stud.*, 1, 1–33.

Bershtein, S., Serohijos, A.W.R., & Shakhnovich, E.I. (2017) Bridging the physical scales in evolutionary biology: From protein sequence space to fitness of organisms and populations. *Curr. Opin. Struct. Biol.*, 42, 31–40.

Bouckaert, R., Heled, J., Kühnert, D., Vaughan, T., Wu, C.H., Xie, D., Suchard, M.A., Rambaut, A., & Drummond, A.J. (2014) BEAST 2: a software platform for Bayesian evolutionary analysis. *PLOS Comput. Biol.*, 10, e1003537.

Chang, K.M. (1992) Dwarf type of *Camaena batanica pancala* (Schmacker and Boettger) from South Cape, Taiwan and its allied species (Pulmonata: Camenidae). *Bull. Malacol.*, 17, 11–20.

Chiba, S. (2005) Appearance of morphological novelty in a hybrid zone between two species of land snail. *Evolution*, 59, 1712–1720.

Davison, A. (2020) Flipping shells! Unwinding LR asymmetry in mirror-image molluscs. *Trends Genet.*, 36, 189–202.

Davison, A., Chiba, S., Barton, N.H., & Clarke, B. (2005) Speciation and gene flow between snails of opposite chirality. *PLOS Biol.*, 3, e282.

Davison, A., McDowell, G.S., Holden, J.M., Johnson, H.F., Koutsovoulos, G.D., Liu, M.M., Hulpiau, P., Van Roy, F., Wade, C.M., Banerjee, R., Yang, F., Chiba, S., Davey, J.W., Jackson, D.J., Levin, M., & Blaxter, M.L. (2016) Formin is associated with left-right asymmetry in the pond snail and the frog. *Curr. Biol.*, 26, 654–660.

Davison, A. & Mordan, P. (2007) A literature database on the mating behavior of stylommatophoran land snails and slugs. *Am. Malacol. Bull.*, 23, 173–181.

Dowling, T.E. & Secor, C.L. (1997) The role of hybridization and introgression in the diversification of animals. *Annu. Rev. Ecol. Syst.*, 28, 593–619.

Drummond, A.J., Ho, S.Y.W., Phillips, M.J., & Rambaut, A. (2006) Relaxed phylogenetics and dating with confidence. *PLOS Biol.*, 4, e88.

Esselstyn, J.A. & Oliveros, C.H. (2010) Colonization of the Philippines from Taiwan: a multi-locus test of the biogeographic and phylogenetic relationships of isolated populations of shrews. *J. Biogeogr.*, 37, 1504–1514.

Excoffier, L., Laval, G., & Schneider, S. (2005) Arlequin (version 3.0): An integrated software package for population genetics data analysis. *Evol. Bioinform. Online*, 1, 47–50.

Excoffier, L., Smouse, P.E., & Quattro, J.M. (1992) Analysis of molecular variance inferred from metric distances among DNA haplotypes: application to human mitochondrial DNA restriction data. *Genetics*, 131, 479–491.

Fehér, Z., Németh, L., Nicoară, A., & Szekeres, M. (2013) Molecular phylogeny of the land snail genus *Alopia* (Gastropoda: Clausiliidae) reveals multiple inversions of chirality. *Zool. J. Linn. Soc.*, 167, 259–272.

Folmer, O., Black, M., Hoeh, W., Lutz, R., & Vrijenhoek, R. (1994) DNA primers for amplification of mitochondrial cytochrome c oxidase subunit I from diverse metazoan invertebrates. *Mol. Mar. Biol. Biotechnol.*, 3, 294–299.

Fukuda, H., Haga, T., & Tatara, Y. (2008) Nikunuki: a useful method for anatomical and DNA studies on shell-bearing molluscs. *Zoosymposia*, 1, 15–38.

Gallagher, S.J., Kitamura, A., Iryu, Y., Itaki, T., Koizumi, I., & Hoiles, P.W. (2015) The Pliocene to recent history of the Kuroshio and Tsushima Currents: a multi-proxy approach. *Prog. Earth Planet. Sci.*, 2, 17.

Giletycz, S., Loget, N., Chang, C.P., & Mouthereau, F. (2015) Transient fluvial

landscape and preservation of low-relief terrains in an emerging orogen: Example from Hengchun Peninsula, Taiwan. *Geomorphology*, 231, 169–181.

Gittenberger, E., Hamann, T.D., & Asami, T. (2012) Chiral speciation in terrestrial pulmonate snails. *PLOS ONE*, 7, e34005.

Grande, C. & Patel, N.H. (2009) Nodal signalling is involved in left–right asymmetry in snails. *Nature*, 457, 1007–1011.

Gude, G.K. (1907) Description of a new species of *Eulota* from Formosa. *Ann. Mag. Nat. Hist. Series 7*, 19, 164–165.

Guillot, G., Mortier, F., & Estoup, A. (2005) Geneland: a computer package for landscape genetics. *Mol. Ecol. Notes*, 5, 712–715.

Hall, R. (2002) Cenozoic geological and plate tectonic evolution of SE Asia and the SW Pacific: computer-based reconstructions, model and animations. *J. Asian Earth Sci.*, 20, 353–431.

Hall, T.A. (1999) BioEdit: a user-friendly biological sequence alignment editor and analysis program for Windows 95/98/NT. *Nucleic Acids Symp. Ser.*, 41, 95–98.

Hammer, O., Harper, D.A.T., & Ryan, P.D. (2001) PAST: Paleontological statistics software package for education and data analysis. *Palaeontol. Electron.*, 4, 1–9.

Harrison, R.G. & Larson, E.L. (2014) Hybridization, introgression, and the nature of species boundaries. *J. Hered.*, 105, 795–809.

Hoang, D.T., Chernomor, O., von Haeseler, A., Minh, B.Q., & Vinh, L.S. (2018) UFBoot2: Improving the ultrafast bootstrap approximation. *Mol. Biol. Evol.*, 35, 518–522.

Hoso, M., Kameda, Y., Wu, S.P., Asami, T., Kato, M., & Hori, M. (2010) A speciation gene for left-right reversal in snails results in anti-predator adaptation. *Nat. Commun.*, 1, 133.

Hsieh, B.C., Wu, S.P., & Tsai, C.L. (2013) *Land Snails of Taiwan*, 3rd ed. Forestry Bureau, Council of Agriculture, Executive Yuan, Taipei, Taiwan.

Huang, C.Y., Yuan, P.B., & Tsao, S.J. (2006) Temporal and spatial records of active arc-continent collision in Taiwan: A synthesis. *Geol. Soc. Am. Bull.*, 118, 274–288.

Huelsenbeck, J.P., Nielsen, R., & Bollback, J.P. (2003) Stochastic mapping of morphological characters. *Syst. Biol.*, 52, 131–158.

Huson, D.H. & Bryant, D. (2006) Application of phylogenetic networks in evolutionary studies. *Mol. Biol. Evol.*, 23, 254–267.

Hwang, C.C. (1995) *Analysis of mitochondrial DNA phylogeny of Camaena* (*Pulmonata: Camaenidae*). Master's dissertation, National Sun Yat-sen University.

Hwang, C.C. (2012) Anatomy and taxonomy of *Satsuma succincta* (Adams, 1866) and *Satsuma batanica pancala* (Schmacker & Boettger, 1891) (Gastropoda: Camaenidae) from southern Taiwan. *Bull. Malacol.*, 35, 1–11.

Hwang, C.C., Ger, M.J., & Wu, S.P. (2022) Within-island diversification in the land snail genus *Formosana* (Gastropoda, Clausiliidae) in Taiwan. *Zool. Scr.*, 51, 562–588.

Hwang, C.C. & Wu, S.P. (2018) Two new species of *Satsuma* A. Adams, 1868 from Taiwan (Pulmonata, Camaenidae). *ZooKeys*, 795, 115–126.

Hwang, C.C., Zhou, W.C., Ger, M.J., Guo, Y., Qian, Z.X., Wang, Y.C., Tsai, C.L., & Wu, S.P. (2021) Biogeography of land snail genus *Acusta* (Gastropoda: Camaenidae): Diversification on East Asian islands. *Mol. Phylogenetics Evol.*, 155, 106999.

ICZN (1999) *International Code of Zoological Nomenclature*, 4th ed. The International Trust for Zoological Nomenclature 1999, London.

Johnson, M.S. (1982) Polymorphism for direction of coil in *Partula suturalis*: Behavioural

isolation and positive frequency dependent selection. *Hered.*, 49, 145–151.

Kaito, T. & Toda, M. (2016) The biogeographical history of Asian keelback snakes of the genus *Hebius* (Squamata: Colubridae: Natricinae) in the Ryukyu Archipelago, Japan. *Biol. J. Linn. Soc. Lond.*, 118, 187–199.

Kalyaanamoorthy, S., Minh, B.Q., Wong, T.K.F., von Haeseler, A., & Jermiin, L.S. (2017) ModelFinder: fast model selection for accurate phylogenetic estimates. *Nat. Methods*, 14, 587–589.

Kao S.I. (2020) *Apatite fission-track dating of the Late Miocene strata* (*Lilungshan Formation*) *in southern Taiwan: Implications for the onset of uplifting of the Hengchun Peninsula*. Master's dissertation, National Taiwan University.

Katoh, K. & Standley, D.M. (2013) MAFFT multiple sequence alignment software version 7: improvements in performance and usability. *Mol. Biol. Evol.*, 30, 772–780.

Kobayashi, S., Usui, R., Nomoto, K., Ushirokita, M., Denda, T., & Izawa, M. (2014) Does egg dispersal occur via the ocean in the stick insect *Megacrania tsudai* (Phasmida: Phasmatidae)? *Ecol. Res.*, 29, 1025–1032.

Koch, E.L., Neiber, M.T., Walther, F., & Hausdorf, B. (2017) High gene flow despite opposite chirality in hybrid zones between enantiomorphic door snails. *Mol. Ecol.*, 26, 3998–4012.

Kramarenko, S. (2014) Active and passive dispersal of terrestrial mollusks: a review. *Ruthenica*, 24, 1–14.

Kuroda, T. (1932) Notes on the land-shell fauna of Kotosho. *Bull. Biogeogr. Soc. Jpn.*, 3, 1–12.

Kuroda, T. & Habe, T. (1949) *Helicacea*. Sanmeisha, Tokyo.

Larsson, A. (2014) AliView: a fast and lightweight alignment viewer and editor for large datasets. *Bioinformatics*, 30, 3276–3278.

Leigh, J.W. & Bryant, D. (2015) POPART: full-feature software for haplotype network construction. *Methods Ecol. Evol.*, 6, 1110–1116.

Lin, C.C. (1974) Mollusks of Lan-Yu (Orchid Island), and their zoogeography. *Bull. Malacol.*, 1, 42–63.

Loo, J.H., Trejaut, J.A., Yen, J.C., Chen, Z.S., Lee, C.L., & Lin, M. (2011) Genetic affinities between the Yami tribe people of Orchid Island and the Philippine Islanders of the Batanes archipelago. *BMC Genet.*, 12, 21.

Maddison, W.P. & Knowles, L.L. (2006) Inferring phylogeny despite incomplete lineage sorting. *Syst. Biol.*, 55, 21–30.

Minato, H. (1988) *A Systematic and Bibliographic List of the Japanese Land Snails*. Nihon Rikusan Kairui Sou-mokuroku Kanko-kai, Shirahama, Japan.

Morii, Y., Yokoyama, J., Kawata, M., Davison, A., & Chiba, S. (2015) Evidence of introgressive hybridization between the morphologically divergent land snails *Ainohelix* and *Ezohelix*. *Biol. J. Linn. Soc.*, 115, 77–95.

Nguyen, L.T., Schmidt, H.A., von Haeseler, A., & Minh, B.Q. (2015) IQ-TREE: A fast and effective stochastic algorithm for estimating maximum-likelihood phylogenies. *Mol. Biol. Evol.*, 32, 268–274.

Orr, H.A. (1991) Is single-gene speciation possible? *Evolution*, 45, 764–769.

Páll-Gergely, B., Hunyadi, A., & Auffenberg, K. (2020) Taxonomic vandalism in malacology: comments on molluscan taxa recently described by N.N. Thach and colleagues (2014–2019). *Folia Malacol.*, 28, 35–76.

Paradis, E. & Schliep, K. (2019) ape 5.0: an environment for modern phylogenetics and evolutionary analyses in R. *Bioinformatics*, 35, 526–528.

Pfeiffer, L. (1866) Descriptions of thirteen new species of land-shells from Formosa, in the collection of the late Hugh Cuming,

collected by Mr. Robert Swinhoe, Vice-Consul of that island. *Proc. Zool. Soc. Lond.*, 1865, 828–831.

R Core Team (2018) R: A Language and Environment for Statistical Computing.

Rambaut, A., Drummond, A.J., Xie, D., Baele, G., & Suchard, M.A. (2018) Posterior summarization in Bayesian phylogenetics using Tracer 1.7. *Syst. Biol.*, 67, 901–904.

Ramírez-Soriano, A., Ramos-Onsins, S.E., Rozas, J., Calafell, F., & Navarro, A. (2008) Statistical power analysis of neutrality tests under demographic expansions, contractions and bottlenecks with recombination. *Genetics*, 179, 555–567.

Richards, P.M., Morii, Y., Kimura, K., Hirano, T., Chiba, S., & Davison, A. (2017) Single-gene speciation: Mating and gene flow between mirror-image snails. *Evol. Lett.*, 1, 282–291.

Ronquist, F., Teslenko, M., van der Mark, P., Ayres, D.L., Darling, A., Höhna, S., Larget, B., Liu, L., Suchard, M.A., & Huelsenbeck, J.P. (2012) MrBayes 3.2: Efficient Bayesian phylogenetic inference and model choice across a large model space. *Syst. Biol.*, 61, 539–542.

Schileyko, A.A. (2004) Treatise on recent terrestrial pulmonate molluscs, Part 12: Bradybaenidae, Monadeniidae, Xanthonychidae, Epiphragmophoridae, Helminthoglyptidae, Elonidae, Humboldtianidae, Sphincterochilidae, Cochlicellidae. *Ruthenica, supplement*, 2, 1627–1763.

Schilthuizen, M., Craze, P.G., Cabanban, A.S., Davison, A., Stone, J., Gittenberger, E., & Scott, B.J. (2007) Sexual selection maintains whole-body chiral dimorphism in snails. *J. Evol. Biol.*, 20, 1941–1949.

Schilthuizen, M., Scott, B.J., Cabanban, A.S., & Craze, P.G. (2005) Population structure and coil dimorphism in a tropical land snail. *Hered.*, 95, 216–220.

Schmacker, B. & Boettger, O. (1891) Neue Materialien zur Charakteristik und geographischen Verbreitung chinesischer und japanischer Binnenmollusken II. *Nachr. Deutsch. Malak. Ges.*, 23, 145–194.

Shih, T.T., Tsai, W.T., Hsu, M.Y., Mezaki, S., & Koba, M. (1989) The study of ages of terraces of coral reef in the Kenting National Park area. (No. 57), Conservation report. Kenting National Park Headquarters, Taiwan.

Shimizu, Y. & Ueshima, R. (2000) Historical biogeography and interspecific mtDNA introgression in *Euhadra peliomphala* (the Japanese land snail). *Hered.*, 85, 84–96.

Sibuet, J.C., Hsu, S.K., Le Pichon, X., Le Formal, J.P., Reed, D., Moore, G., & Liu, C.S. (2002) East Asia plate tectonics since 15 Ma: constraints from the Taiwan region. *Tectonophysics*, 344, 103–134.

Simon, B.C., Frati, F., Beckenbach, A., Crespi, B., Liu, H., & Flook, J.P. (1994) Evolution, weighting, and phylogenetic utility of mitochondrial gene sequences and a compilation of conserved polymerase chain reaction primers. *Ann. Entomol. Soc. Am.*, 87, 651–701.

Sinagawa, K. (1979) Anatomy of *Camaena cicatricosa*, *Pancala bacca* and *Pancala batanica pancala*. *Kainakama*, 13, 4–7.

Tabe, M. (1937) Morphological study of *Coniglobus batanicus pancalus* (Schmacker & Boettger) and *C. b. boteltobagoensis* Kuroda and on the systematic position of the genus *Coniglobus*. *Zoological Magazine*, 49, 12–20.

Tamura, K. & Nei, M. (1993) Estimation of the number of nucleotide substitutions in the control region of mitochondrial DNA in humans and chimpanzees. *Mol. Biol. Evol.*, 10, 512–526.

Thach, N.N. (2021) *New Shells of South Asia and Taiwan, China, Tanzania. Seashells*Freshwater*Land Snails. With 116 New Species and*

Subspecies and Rejected Synonyms, Accepted Species. 48HRBooks Company, Akron, Ohio, USA.

Truett, G.E., Heeger, P., Mynatt, R.l., Truett, A.A., Walker, J.A., & Warman, M.L. (2000) Preparation of PCR-quality mouse genomic DNA with hot sodium hydroxide and tris (HotSHOT). *BioTechniques*, 29, 52–54.

Tseng, H.Y., Huang, W.S., Jeng, M.L., Villanueva, R.J.T., Nuñeza, O.M., & Lin, C.P. (2018) Complex inter-island colonization and peripatric founder speciation promote diversification of flightless *Pachyrhynchus* weevils in the Taiwan–Luzon volcanic belt. *J. Biogeogr.*, 45, 89–100.

Ueshima, R. & Asami, T. (2003) Single-gene speciation by left–right reversal. *Nature*, 425, 679–679.

Wang, P., Xiao, Q., Zhou, W.C., & Hwang, C.C. (2014) Revision of three camaenid and one bradybaenid species (Gastropoda, Stylommatophora) from China based on morphological and molecular data, with description of a new bradybaenid subspecies from Inner Mongolia, China. *Zookeys*, 372, 1–16.

Wu, S.P., Hwang, C.C., & Lin, Y.S. (2008) Systematic revision of the arboreal snail *Satsuma albida* species complex (Mollusca: Camaenidae) with descriptions of 14 new species from Taiwan. *Zool. J. Linn. Soc.*, 154, 437–493.

Xia, X. (2018) DAMBE7: new and improved tools for data analysis in molecular biology and evolution. *Mol. Biol. Evol.*, 35, 1550–1552.

Xia, X., Xie, Z., Salemi, M., Chen, L., & Wang, Y. (2003) An index of substitution saturation and its application. *Mol. Phylogenetics Evol.*, 26, 1–7.